nature
structural biology

Bistable regulation of integrin adhesiveness by a bipolar metal ion cluster

JianFeng Chen, Azucena Salas & Timothy A Springer

Integrin $\alpha_4\beta_7$ mediates rolling adhesion in Ca^{2+} and Ca^{2+} + Mg^{2+}, and firm adhesion in Mg^{2+} and Mn^{2+}, mimicking the two key steps in leukocyte accumulation in inflamed vasculature. We mutated an interlinked linear array of three divalent cation-binding sites present in integrin β-subunit I-like domains. The middle, metal ion–dependent adhesion site (MIDAS) is required for both rolling and firm adhesion. One polar site, that adjacent to MIDAS (ADMIDAS), is required for rolling because its mutation results in firm adhesion. The other polar site, the ligand-induced metal binding site (LIMBS), is required for firm adhesion because its mutation results in rolling. The LIMBS mediates the positive regulatory effects of low Ca^{2+} concentrations, whereas the ADMIDAS mediates the negative regulatory effects of higher Ca^{2+} concentrations, which are competed by Mn^{2+}. The bipolar sites thus stabilize two alternative phases of adhesion.

Metal ions regulate the activity of many enzymes and receptors, including integrins, a family of heterodimeric cell surface receptors for cell surface and extracellular matrix ligands[1]. Global conformational changes in extracellular domains that regulate integrin adhesiveness have recently been revealed by atomic and high-resolution electron microscopy (EM) structures, and multiple metal ion–binding sites have been defined in crystal structures[1–8]. Nonetheless, long-standing observations that metal ions regulate adhesion by integrins[9–15] remain unexplained. As compared with results in Mg^{2+} + Ca^{2+}, addition of Mn^{2+} or removal of Ca^{2+} strikingly increases ligand binding affinity and adhesiveness of almost all integrins. In addition to these quantitative differences, studies on α_4 integrins have revealed qualitative differences in adhesion in shear flow[16–18]. In Ca^{2+}, $\alpha_4\beta_7$ mediates rolling adhesion, whereas in Mg^{2+} alone and in Mn^{2+}, $\alpha_4\beta_7$ mediates firm adhesion on its ligand mucosal addressin cell adhesion molecule-1 (MAdCAM-1), mimicking the two key steps in leukocyte accumulation in the vasculature at inflammatory sites[18]. Early studies on integrins revealed metal-binding sites in the α-subunit β-propeller domain and I domain[19], but mutational studies suggested that they were not responsible for the regulatory effects of Ca^{2+} and Mn^{2+} (refs. 1,20–22).

A liganded crystal structure of integrin $\alpha_V\beta_3$ revealed a remarkable linear array of three divalent cation-binding sites centered on the ligand-binding site in the β-subunit I-like domain (**Fig. 1a**)[7,8]. The middle site, called the metal ion–dependent adhesion site (MIDAS) because its metal ion directly coordinates the side chain of the acidic residue characteristic of all integrin ligands, and the two outer sites, ADMIDAS and LIMBS, are all formed by loops at the C-terminal end of the central hydrophobic β-sheet in the three-layer α-β-α Rossmann fold of the I-like domain. The sites line up along the ends of the β-strands, which are ordered 3-2-1-4-5-6, with the β2-β3 and β6-α7 loops on opposite sides of the β-sheet contributing coordinations to the LIMBS and ADMIDAS poles of the triple site (**Fig. 1a**,**b**). In Ca^{2+} and in the absence of a ligand, only the ADMIDAS is occupied (**Fig. 1b**), whereas in Mn^{2+} and a ligand-mimetic peptide all three sites bind metal ions (**Fig. 1a**), and there are substantial shifts in position of MIDAS and ADMIDAS coordinating residues[7,8] (**Fig. 1a**,**b**). Both $\alpha_V\beta_3$ structures are present in a highly bent conformation, and the liganded $\alpha_V\beta_3$ structure was obtained by soaking ligand and Mn^{2+} into unliganded crystals formed in Ca^{2+} (refs. 7,8). By contrast, when ligand is added to $\alpha_V\beta_3$ when it is free in solution or on the cell surface, a switchblade-like motion occurs that extends the ligand-binding headpiece much farther above the cell surface, and other conformational changes occur in the ligand-binding site that increase its affinity for ligand[5,6]. To mediate rolling adhesion, it seems that integrins adopt an extended conformation[23], and the extended conformation also mediates firm adhesion as shown by ligand-induced binding site epitopes that are exposed[3,5]. In the extended conformation, two different conformations of the integrin headpiece have been observed that differ in the angle between the β-subunit I-like and hybrid domains, and in ligand binding affinity. Furthermore, these conformations are speculated to differ in the structure of the metal-binding sites in the I-like domain[5,6]. It is possible that the closed and open conformations of the headpiece could mediate rolling and firm adhesion, respectively.

Integrin $\alpha_4\beta_7$ is critical for homing of lymphocytes to the intestine and associated lymphoid tissue, such as Peyer's patches[24,25]. Its ligand, MAdCAM-1, is a glycoprotein in the Ig superfamily and is expressed on endothelia in mucosal tissue and Peyer's patches[26]. Integrin $\alpha_4\beta_7$ mediates rolling of lymphocytes on vessels bearing MAdCAM-1, and after activation, firm adhesion[16,18,25]. Rolling and firm adhesion seem

The CBR Institute of Biomedical Research and Department of Pathology, Harvard Medical School, Boston, Massachusetts 02115, USA. Correspondence should be addressed to T.A.S. (springeroffice@cbr.med.harvard.edu).

Published online 9 November 2003; doi:10.1038/nsb1011

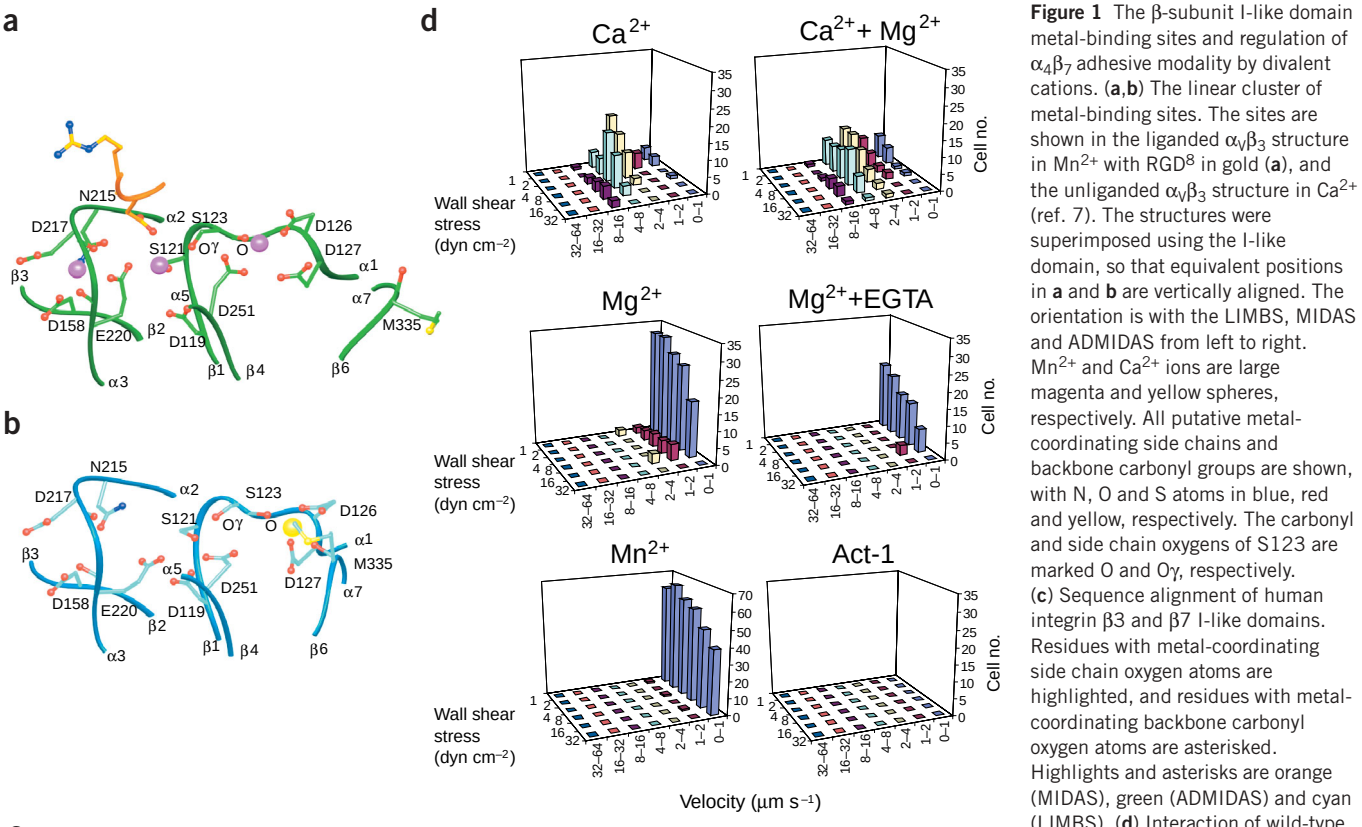

Figure 1 The β-subunit I-like domain metal-binding sites and regulation of $\alpha_4\beta_7$ adhesive modality by divalent cations. (**a**,**b**) The linear cluster of metal-binding sites. The sites are shown in the liganded $\alpha_V\beta_3$ structure in Mn^{2+} with RGD[8] in gold (**a**), and the unliganded $\alpha_V\beta_3$ structure in Ca^{2+} (ref. 7). The structures were superimposed using the I-like domain, so that equivalent positions in **a** and **b** are vertically aligned. The orientation is with the LIMBS, MIDAS and ADMIDAS from left to right. Mn^{2+} and Ca^{2+} ions are large magenta and yellow spheres, respectively. All putative metal-coordinating side chains and backbone carbonyl groups are shown, with N, O and S atoms in blue, red and yellow, respectively. The carbonyl and side chain oxygens of S123 are marked O and Oγ, respectively. (**c**) Sequence alignment of human integrin β3 and β7 I-like domains. Residues with metal-coordinating side chain oxygen atoms are highlighted, and residues with metal-coordinating backbone carbonyl oxygen atoms are asterisked. Highlights and asterisks are orange (MIDAS), green (ADMIDAS) and cyan (LIMBS). (**d**) Interaction of wild-type $\alpha_4\beta_7$ 293T cell transfectants with MAdCAM-1 substrates. Cells were infused into the flow chamber in buffer containing 1 mM Ca^{2+}, 1 mM Ca^{2+} + 1 mM Mg^{2+}, 1 mM Mg^{2+}, 2 mM Mg^{2+} + 1 mM EGTA, or 0.5 mM Mn^{2+}. Rolling velocities of individual cells were measured at a series of increasing wall shear stresses, and cells within a given velocity range were enumerated to give the population distribution.

to be two distinct phases of adhesion, with a phase transition between them[27], raising the question of whether there is a clear molecular basis for bistable regulation of the adhesive modality. We have mutated metal ion–binding residues to define the function of the LIMBS, MIDAS and ADMIDAS sites. The LIMBS functions as a positive regulatory site required for firm adhesion and positive effects of low Ca^{2+} concentrations. The ADMIDAS functions as a negative regulatory site required for rolling adhesion. It seems to mediate the negative regulatory effect of high Ca^{2+} concentrations, which are competed by Mn^{2+}. The MIDAS is required for both rolling and firm adhesion, and seems to adopt two alternative conformations that mediate the rolling and firm phases of adhesion that are stabilized by the bipolar LIMBS and ADMIDAS sites.

RESULTS

Adhesion in shear flow of $\alpha_4\beta_7$ mutants

To test the function of the LIMBS, MIDAS and ADMIDAS sites in regulating the transition between the rolling and firm phases of adhesion, they were mutated in $\alpha_4\beta_7$. The I-like domain is highly conserved in integrin β subunits, with 52% amino acid sequence identity between β_3 and β_7, and identity in all residues with side chains coordinating to the LIMBS, MIDAS and ADMIDAS metal ions (**Fig. 1c**). Because of this high identity in sequence and absolute identity in coordinating side chains, we assume that the β_3 structure is an excellent model for understanding the effect of β_7 mutations. Although β_3 integrins are not known to mediate rolling, both the $\alpha_4\beta_7$ and $\alpha_4\beta_1$ integrins mediate rolling[16,17], despite one difference between β_1 and β_7 in a LIMBS coordinating side chain. We believe that any differences between β_3 and β_7 in metal ion coordination are likely to be lesser than differences in metal ion coordination between the bent and extended integrin conformations. We use the β_3 sequence numbering for β_7 mutations here (**Table 1**) to simplify referring to the β3 structure for the effect of β7 mutations (**Fig. 1a**,**b**).

Adhesive behavior in shear flow of 293T transient or K562 stable $\alpha_4\beta_7$ transfectants was characterized in a parallel wall flow chamber with MAdCAM-1 adsorbed to its lower wall. Cells were allowed to accumulate at a wall shear stress of 0.3 dyn cm^{-2}. The shear stress was incrementally increase every 10 s and the velocity of the cells remaining bound at each increment was determined. Wild-type 293T transfectants behaved as previously described for lymphoid cells expressing

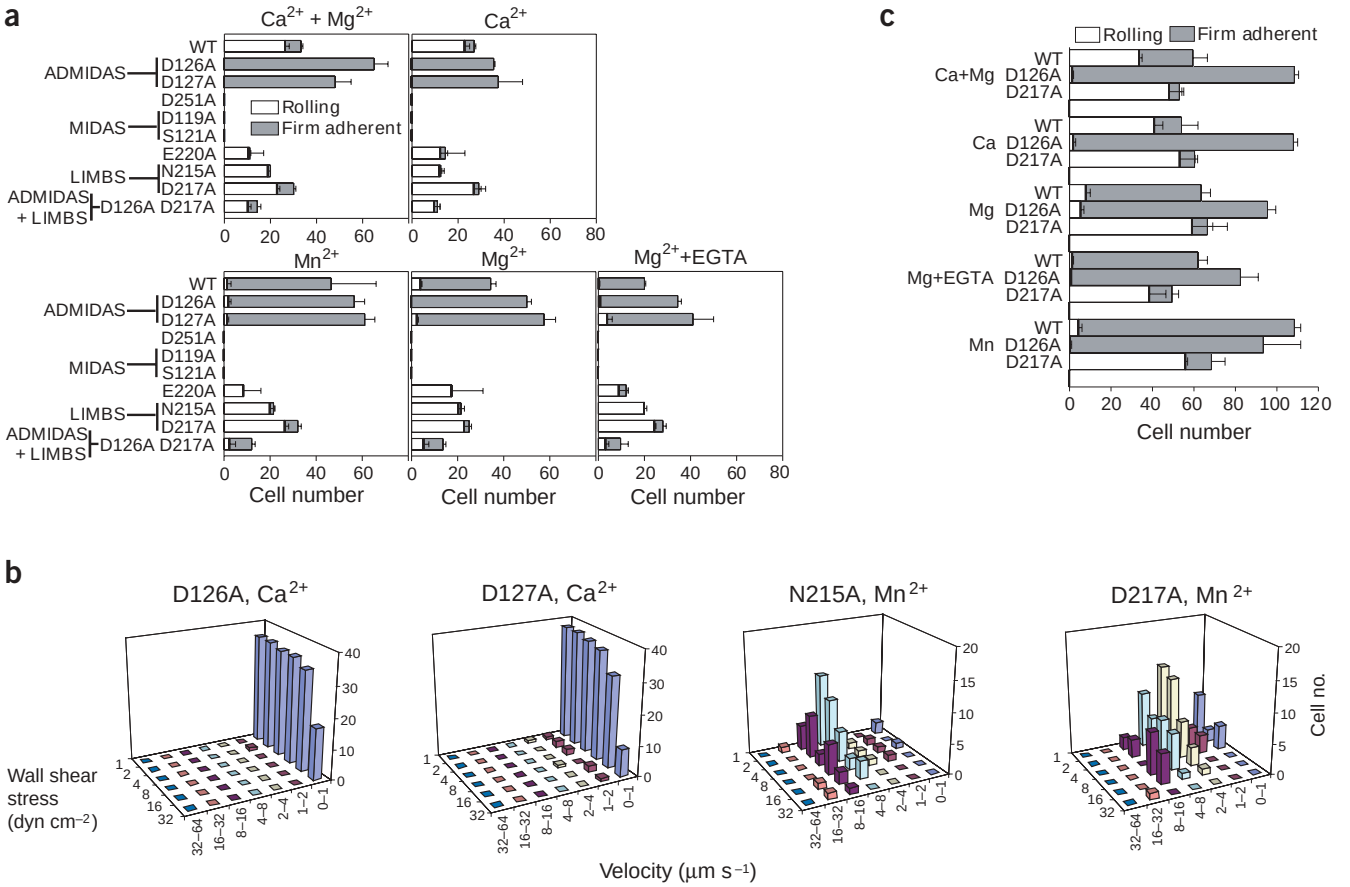

Figure 2 Effect of the metal ion–binding site mutations on the adhesive modality of $\alpha_4\beta_7$ and resistance to detachment in shear flow. (**a**–**c**) Rolling and firm adhesion on MAdCAM-1 substrates of 293T transfectants (**a**,**b**) and K562 transfectants (**c**). The number of rolling and firmly adherent wild-type and mutant $\alpha_4\beta_7$ transfectants containing the indicated β I-like mutations was measured in the indicated divalent cations at a wall shear stress of 1 dyn cm^{-2} (**a**,**c**) or rolling velocity was measured for all cells and plotted as a distribution over a range of wall shear stresses (**b**). All experiments used the metal ion concentrations described in the legend to **Figure 1**, and data are shown ±s.d. ($n = 3$).

$\alpha_4\beta_7$ (ref. 18) (**Fig. 1d**). In 1 mM Ca^{2+} or 1 mM Ca^{2+} + 1 mM Mg^{2+}, cells rolled with increasing velocity as shear stress was increased, reaching a velocity of ~8 μm s^{-1} at 16 dyn cm^{-2}, and were mostly detached at 32 dyn cm^{-2} (**Fig. 1d**). By contrast, cells were firmly adherent in 1 mM Mg^{2+} and 2 mM Mg^{2+} + 1 mM EGTA (**Fig. 1d**). In Mn^{2+}, more cells accumulated and shear resistance at 32 dyn cm^{-2} was increased (**Fig. 1d**). Cells transfected with the α_4 cDNA alone, or $\alpha_4\beta_7$ transfectants treated with the Act-1 monoclonal antibody to $\alpha_4\beta_7$ or with 5 mM EDTA, did not accumulate on MAdCAM-1 substrates (**Fig. 1d** and data not shown).

All β_7 metal-coordinating ADMIDAS and LIMBS side chains, and representative MIDAS side chains, were mutated to alanine. Of nine single mutants and one double mutant, all were well expressed except for E158A (**Table 1**). Each of two MIDAS mutants, D119A and S121A, completely abolished adhesion, independent of the divalent cation conditions (**Fig. 2a**). Thus, not only Mg^{2+}- and Mn^{2+}-dependent firm adhesion, but also Ca^{2+}-dependent rolling adhesion, requires the MIDAS.

ADMIDAS and LIMBS mutants act in opposite ways

The two ADMIDAS mutants, D126A and D127A, both showed the same surprising behavior. Regardless of the divalent cations, these mutants supported only firm adhesion in 293T transfectants (**Fig. 2a**). The firm adhesion in Ca^{2+} of the D126A and D127A mutants (**Fig. 2b**) was diametrically opposed to the wild-type behavior of rolling in Ca^{2+} (**Fig. 1d**). The same results were seen with a representative ADMIDAS mutant, D126A, in K562 cell transfectants (**Fig. 2c**). Furthermore, in all divalent cations except Mn^{2+}, accumulation of ADMIDAS mutants on MAdCAM-1 substrates—that is, the total number of rolling and firmly adherent cells—was greater than wild type (**Fig. 2a**,**c**). Substitution of Mn^{2+} for other divalent cations did not further augment adhesion by ADMIDAS mutants, and adhesion of ADMIDAS mutants in all divalent cations was similar to that of wild type in Mn^{2+} (**Fig. 2a**,**c**), showing that the ADMIDAS mutants are fully activated, and that ADMIDAS mutations and Mn^{2+} have functionally equivalent and nonadditive effects.

The LIMBS mutants showed a similarly surprising but opposite behavior. Regardless of the divalent cations, the LIMBS mutants mediated only rolling (**Fig. 2a** and **Table 1**). For example, the N215A and D217A mutants rolled in Mn^{2+} (**Fig. 2b**) in contrast to firm adhesion by wild-type $\alpha_4\beta_7$ in Mn^{2+} (**Fig. 1d**). Similar results were obtained with a representative LIMBS mutant, D217A, in K562 transfectants (**Fig. 2c**).

To compare results for $\alpha_4\beta_7$ to those for other integrins where the influence of metal ions on strength of adhesion to substrates is reported, we examined resistance to detachment by increasing shear (**Fig. 3**). The data demonstrate that ADMIDAS mutants augment

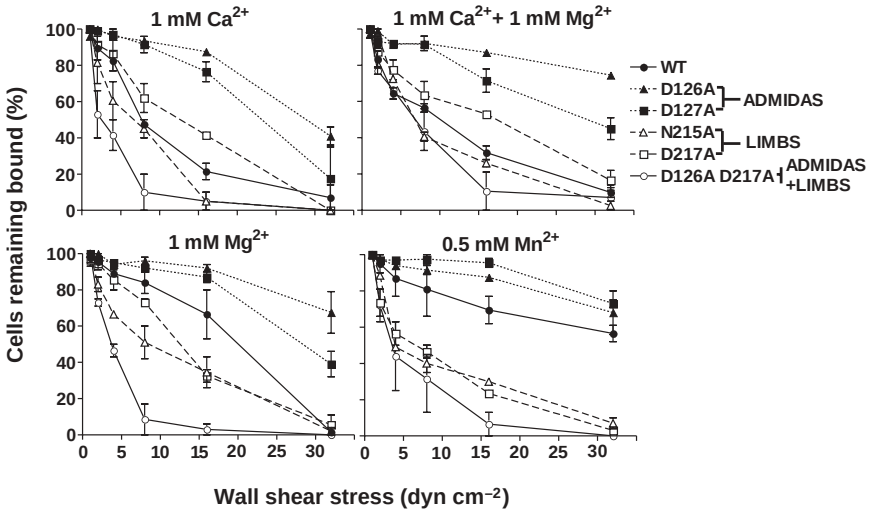

Mutants	Initial bound cell number			
	Ca^{2+}	Ca^{2+} + Mg^{2+}	Mg^{2+}	Mn^{2+}
WT	30 ± 5	33 ± 3	35 ± 3	69 ± 0
D126A	36 ± 1	65 ± 6	50 ± 2	57 ± 6
D127A	40 ± 9	48 ± 7	58 ± 6	61 ± 4
N215A	12 ± 2	20 ± 1	21 ± 2	22 ± 1
D217A	29 ± 6	30 ± 2	25 ± 1	32 ± 0
D126A D217A	6 ± 3	13 ± 1	11 ± 4	12 ± 4

Figure 3 Resistance to detachment. The total number of cells remaining rollingly or firmly adherent at increasing wall shear stresses was determined as a percent of adherent cells at 1 dyn cm^{-2}. The initial number of bound cells at 1 dyn cm^{-2} is shown below. Data are from the same experiments with 293T transfectants described in the **Figure 2** legend, and are ±s.d. ($n = 3$).

adhesion relative to wild type as Mn^{2+} does in general for integrins, and that LIMBS mutants restrain augmentation of adhesion by Mg^{2+} and Mn^{2+}, as Ca^{2+} does for most integrins.

Intermediate position residues

Two residues have side chains located between two metal ion–binding sites. The Glu220 side chain coordinates both the LIMBS and MIDAS metal ions in the liganded, bent $\alpha_V\beta_3$ structure (**Fig. 1a**). Interestingly, the E220A mutant shows the same rolling phenotype as the Asn215 and Asp217 LIMBS mutants and is competent for ligand binding, in strong contrast to the Asp119 and Ser121 MIDAS mutants. Thus, although Glu220 has been previously considered to be a MIDAS residue in the bent, unliganded structure[7], or both a MIDAS and LIMBS residue in the bent, liganded structure[8], it behaves functionally like a LIMBS residue in the presumably extended conformation of $\alpha_4\beta_7$ that mediates firm adhesion.

The Asp251 side chain is located intermediately between the MIDAS and ADMIDAS sites (**Fig. 1a**,**b**). In the unliganded $\alpha_V\beta_3$ structure in Ca^{2+}, its side chain orients toward the unoccupied MIDAS site[7] (**Fig. 1b**), whereas in the liganded $\alpha_V\beta_3$ structure in Mn^{2+}, its side chain coordinates the ADMIDAS metal ion[8] (**Fig. 1a**). Functionally, in $\alpha_4\beta_7$ the Asp251 mutant behaves like the MIDAS mutants (**Fig. 2a** and **Table 1**).

The findings for both intermediately positioned residues suggest some coordination differences between the liganded, bent $\alpha_V\beta_3$ crystal structure and the physiologically liganded, extended $\alpha_4\beta_7$. As explained above, we think that this reflects coordination differences between integrins in the bent conformation and in the extended conformations thought to mediate rolling and firm adhesion[5,23], although we cannot exclude differences between $\alpha_V\beta_3$ and $\alpha_4\beta_7$. Results with Asp217 are also consistent with rearrangement at the LIMBS. In the published figures for the liganded $\alpha_V\beta3$ crystal structure in ref. 8, the Asp217 side chain coordinates the LIMBS metal, but in PDB entry 1L5G the side chain has a different orientation, pointing away from the LIMBS metal ion (**Fig. 1a**). In $\alpha_4\beta_7$, Asp217 behaves functionally as a LIMBS residue, suggesting that it coordinates the LIMBS metal ion in the extended conformation that mediates the firm adhesion modality.

Double mutants

The double ADMIDAS and LIMBS mutant D126A D217A mediated adhesion, although this was decreased compared to wild type (**Figs. 2a** and **3**). This result is consistent with the lowered expression level of this mutant (**Table 1**). The ability of the double mutant to function shows that the MIDAS is sufficient for adhesion, and the results in Ca^{2+}, Mg^{2+} or Mn^{2+} alone suggest that each of these ions can bind to the MIDAS and coordinate with ligand.

Positive and negative regulation by Ca^{2+}

For most integrins, Ca^{2+} has both positive and negative regulatory effects. Low, ~0.1 mM concentrations of Ca^{2+} augment adhesion at

Table 1 Expression and adhesive modality of $\alpha_4\beta_7$ mutants

	Mutated residue[a]	Expression[b] (% WT)	Ca^{2+} + Mg^{2+}	Ca^{2+}	Mn^{2+}	Mg^{2+}	Mg^{2+} + EGTA
			Rolling cells (%)[c]				
	WT	100 ± 12	80	85	2	12	2
ADMIDAS	Asp126	70 ± 9	0	0	4	0	3
ADMIDAS	Asp127	115 ± 17	0	0	2	4	9
	Asp251	90 ± 10	–	–	–	–	–
MIDAS	Asp119	56 ± 14	–	–	–	–	–
MIDAS	Ser121	48 ± 5	–	–	–	–	–
	Glu220	107 ± 21	95	96	100	100	85
LIMBS	Asn215	153 ± 20	95	96	93	95	100
LIMBS	Asp217	99 ± 20	77	93	80	92	88
LIMBS	Glu158	24 ± 3	–	–	–	–	–
ADMIDAS + LIMBS	Asp126 + Asp217	51 ± 15	73	100	21	57	50

[a]The β_3 residue numbering is used for β_7 mutations. All corresponding residues are identical, and for β_3:β_7 are 119:140, 121:142; 126:147; 127:148; 158:179; 215:235; 217:237; 220:240 and 251:270. All mutations are to alanine. [b]Integrin $\alpha_4\beta_7$ cell surface expression in 293T transient transfectants compared with wild type determined with Act-1 monoclonal antibody and immunofluorescence flow cytometry. The data represent mean fluorescence intensity ± difference from the mean for two independent experiments. [c]The percent of total adherent 293T transfectants that roll at a wall shear stress of 1 dyn cm^{-2}. Dash indicates that no adherent cells were observed.

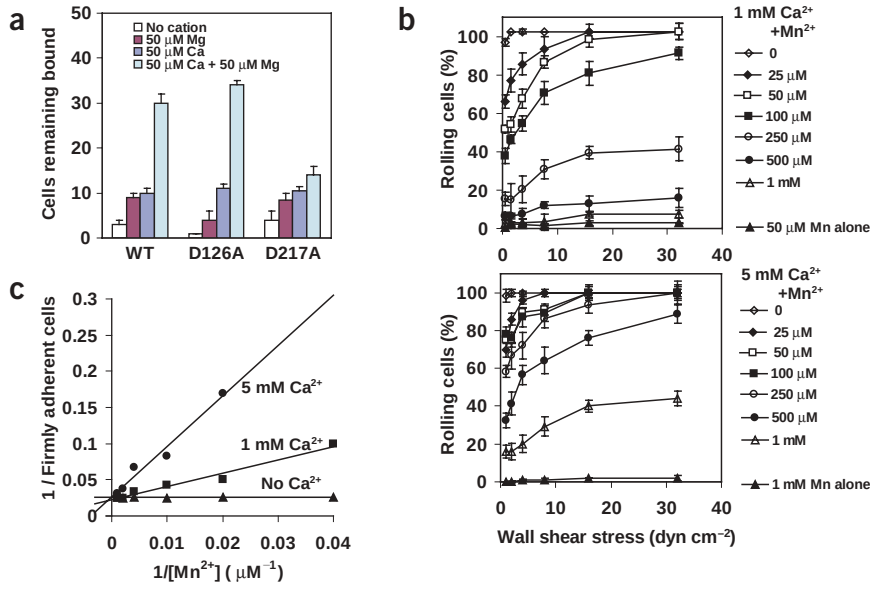

Mn^{2+} (μM)	25	50	100	250	500	1,000
No Ca^{2+}	38 ± 7	38 ± 8	40 ± 3	38 ± 5	40 ± 8	38 ± 10
1 mM Ca^{2+}	10 ± 2	20 ± 3	23 ± 3	29 ± 5	40 ± 4	40 ± 9
5 mM Ca^{2+}	5 ± 2	6 ± 2	12 ± 3	15 ± 2	26 ± 4	32 ± 7

Figure 4 Positive and negative regulation of $\alpha_4\beta_7$ by Ca^{2+} and competition between Ca^{2+} and Mn^{2+}. (**a**) Synergistic effect of low concentrations of Ca^{2+} and Mg^{2+} on the adhesion of K562 transfectants on MAdCAM-1. The number of adherent cells was measured in 50 μM of the indicated divalent cations at a wall shear stress of 2 dyn cm^{-2}. (**b**) Effect of 1 mM Ca^{2+} (upper) and 5 mM Ca^{2+} (lower) on firm adhesion stimulated by varying concentrations of Mn^{2+}. The total number of wild-type $\alpha_4\beta_7$ 293T transfectants remaining rollingly and firmly adherent on MAdCAM-1 at different wall shear stresses was measured and the percentage of rolling cells was calculated at each wall shear stress. (**c**) Double-reciprocal plot of the number of firmly adherent cells versus Mn^{2+} concentration in the presence of 0, 1 and 5 mM Ca^{2+} at a wall shear stress of 1 dyn cm^{-2}. Linear regression fits show that the three lines intersect on the *y*-axis, demonstrating competitive inhibition of Mn^{2+}-stimulated firm adhesion by Ca^{2+}. The number of firmly adherent cells plotted in **c** is shown in the table. All data are shown ±s.d. ($n = 3$).

suboptimal ~0.1 mM Mg^{2+} concentrations, whereas higher 1–10 mM concentrations of Ca^{2+} inhibit adhesion at optimal ~1 mM Mg^{2+} concentrations[9,11,13]. Similarly, for $\alpha_4\beta_7$, low concentrations of Ca^{2+} greatly augmented adhesion in 50 μM Mg^{2+} (**Fig. 4a**). Synergistic adhesion in 50 μM Ca^{2+} + 50 μM Mg^{2+} compared with either divalent cation alone was seen with the wild type and D126A ADMIDAS mutant, but not with the D217A LIMBS mutant (**Fig. 4a**). Therefore, positive regulation by low concentrations of Ca^{2+} requires the LIMBS but not the ADMIDAS, and reflects interactions between Ca^{2+} and Mg^{2+} at the LIMBS and MIDAS.

The requirement for the LIMBS for positive regulation by Ca^{2+} in low concentrations of Mg^{2+}, and the finding that the ADMIDAS is a negative regulatory site, and that its removal by mutation resembles the effect of removal of Ca^{2+} when Mg^{2+} is sufficient, suggest that the negative regulatory site for Ca^{2+} is the ADMIDAS. Ca^{2+} and Mn^{2+} could exert their negative and positive effects by binding to distinct sites (noncompetitively) or the same site (competitively). These negative and positive effects result from binding to the same site, because firm adhesion stimulated by Mn^{2+} could always be altered to rolling adhesion through competition by Ca^{2+} (**Fig. 4b**). Furthermore, competition by Ca^{2+} at varied Mn^{2+} concentrations showed that the proportion of rolling cells was determined by the ratio of the Ca^{2+} and Mn^{2+} concentrations, as predicted by competitive inhibition (**Fig. 4b**). Moreover, double-reciprocal plots of the number of firmly adherent cells and Mn^{2+} concentration intersected on the *y*-axis, confirming competitive inhibition (**Fig. 4c**).

DISCUSSION

Bistable regulation of integrins

Our results demonstrate a notably clear-cut mechanism for bistable regulation of the rolling and firm phases of integrin adhesiveness. Bistability is enforced by a novel bipolar metal ion cluster in which the metal ion–binding sites at each pole of the linear cluster have opposite effects on ligand binding to the central metal ion site. Binding of Ca^{2+} and Mg^{2+} to the LIMBS and MIDAS stabilizes a conformation and metal coordination geometry that mediates firm adhesion, whereas binding of these metals to the MIDAS and ADMIDAS stabilizes an alternative conformation and coordination state that mediates rolling adhesion. Bistable regulation is biologically important to enable $\alpha_4\beta_7$ on lymphocytes to switch between the rolling on endothelium required for surveillance of inflammatory stimuli, and the firm adhesion required for localization in a vascular bed and subsequent diapedesis. The rolling and firm phases of adhesion by $\alpha_4\beta_7$ are a consequence of fast and slow dissociation rate constants from MAdCAM-1 (ref. 18), and therefore can be equated to weak and strong adhesion by other integrins, in agreement with the correlation demonstrated here of rolling and firm adhesion with low and high resistance to detachment in shear, respectively. Thus, the ADMIDAS and LIMBS are negative and positive regulatory sites, respectively, that determine whether the MIDAS has low or high affinity for ligand. Minor discrepancies between current integrin crystal structures and the phenotypes of the mutants of Asp251, Glu20 and Asp217 suggest that alterations in their metal ion coordinations may occur between the bent low-affinity integrin conformation and the extended conformations that mediate rolling and firm adhesion, although we cannot rule out differences in coordination among the integrin β_3 and β_7 subunits.

The LIMBS

Overall, our results are in excellent agreement with integrin crystal and EM structures[5–8], and provide a unifying view of how the LIMBS and ADMIDAS sites interact with metal ions in bipolar regulation of integrin function. Mutation of the LIMBS shows that its occupancy positively regulates ligand binding by integrins, as confirmed by its requirement for positive regulation of ligand binding by low concentrations of Ca^{2+}. In agreement, in $\alpha_V\beta3$ crystal structures, metal ions are found bound to the LIMBS and MIDAS sites when ligand is bound, but not when Ca^{2+} or Mn^{2+} alone is present[7,8]. As ligand binding enhances metal ion binding at the LIMBS and MIDAS, metal ion bind-

ing to these sites must also enhance ligand binding. Our data demonstrate that at low concentrations of Ca^{2+} and Mg^{2+}, one of these metal ions preferentially binds to the LIMBS and the other to the MIDAS. Because of the chemistry of the coordinating oxygen atoms at these sites, Ca^{2+} is predicted to have higher affinity than Mg^{2+} for the LIMBS. The LIMBS has two backbone and one amide side chain carbonyl O coordinations, whereas the MIDAS has no carbonyl O coordinations. Calcium has a far greater propensity than Mg^{2+} to form backbone carbonyl O coordinations, as shown by examination of a large number of high-resolution crystal structures[28]. It thus seems that the LIMBS is occupied by Ca^{2+} at low concentrations and the MIDAS is occupied by Mg^{2+} at low concentrations.

The ADMIDAS

Mutation of the ADMIDAS shows that its occupancy can negatively regulate integrins. As Ca^{2+} is the only divalent cation known to negatively regulate integrins, and the LIMBS is ruled out because it is a positive regulatory site for Ca^{2+}, we conclude that the ADMIDAS is the negative regulatory site responsible for inhibition by high concentrations of Ca^{2+}. Furthermore, Mn^{2+} activates by competing with Ca^{2+} at this site. The competing activities of Mn^{2+} and Ca^{2+} at the ADMIDAS are readily explicable in terms of integrin crystal and EM structures[5–8] and the chemistry of these ions. In the $\alpha_V\beta_3$ structure in Ca^{2+}, the backbone carbonyl oxygen of Met335 in the β6-α7 loop of the I-like domain forms one of the coordinations to the Ca^{2+} ion at the ADMIDAS (**Fig. 1b**). In contrast, in the liganded $\alpha_V\beta_3$ structure in Mn^{2+}, the Mn^{2+} ion at the ADMIDAS shifts 4 Å toward the LIMBS pole, and Met335 shifts away in the opposite direction (**Fig. 1a**,**b**). Loss of the Met335 carbonyl coordination is favored by substitution of Mn^{2+} for Ca^{2+}, because Ca^{2+} but not Mn^{2+} has a strong propensity to coordinate carbonyl oxygen atoms[28]. The I-like domain α7 helix appears to move axially during integrin activation[5,6], pulling the β6-α7 loop away from the ADMIDAS, and thus loss of the coordination to Met335 in the β6-α7 loop seems to be a key step in the integrin activation pathway.

Bipolar regulation of the MIDAS

The findings suggest that the central MIDAS metal ion has two alternative coordination geometries, one stabilized by ADMIDAS occupation by Ca^{2+} that mediates rolling adhesion, and another stabilized by LIMBS occupation that mediates firm adhesion. Notably, the axis of the three metal ion–binding sites is aligned perpendicularly to the interface between the α-subunit β-propeller domain and the β-subunit I-like domain, where ligand is bound, with the LIMBS pole adjacent to and pointing to the β-propeller. Displacement of the ADMIDAS metal ion toward the LIMBS along this axis regulates integrin activation. Further structural work will be required to determine the exact coordination status of the metal ion cluster when it mediates firm and rolling adhesion in the extended integrin conformation. The $\alpha_V\beta3$ structures determined to date are of bent structures and have either all three sites occupied or only the ADMIDAS occupied (**Fig. 1a**,**b**)[7,8]. The configuration that mediates rolling adhesion probably occurs in the extended conformation with the closed headpiece[5,6] and appears to most resemble that of the Ca^{2+}-bound, unliganded structure with the backbone carbonyl ligand donated from the β6-α7 loop (**Fig. 1b**), but the MIDAS must also be occupied. The system of metal ion coordinations that mediates firm adhesion appears to most resemble the ligand-bound configuration with three metal ions bound (**Fig. 1a**), but our results suggest that some further subtle changes are likely to occur between the liganded, bent conformation observed in the $\alpha_V\beta3$ crystal structure and the extended, high-affinity conformation with the open headpiece that mediates firm adhesion[5,6].

METHODS

cDNA construction and expression. The β_7 site-directed mutations were generated using QuikChange (Stratagene). Wild-type human β_7 cDNA[29] in vector pcDNA3.1/Hygro(–) (Invitrogen) was used as the template. All mutations were confirmed by DNA sequencing.

Transient transfection of 293T and stable transfection of K562 cells were done as described[30,31]. Wild-type human integrin $\alpha_4\beta_7$ K562 stable transfectant (K562-$\alpha_4\beta_7$) was a gift from D.J. Erle[29]. KA4, a K562 cell line stably transfected with human integrin α_4 (ref. 32), was retransfected with mutated human β_7 and selected with hygromycin and G418 to make K562 stable transfectants.

Flow cytometry. Immunofluorescence flow cytometry was done as described[31]. Act-1 monoclonal antibody specific for integrin $\alpha_4\beta_7$ was previously described[33,34].

Flow chamber assay. A polystyrene Petri dish was coated with a 5 mm–diameter, 20-μl spot of 5 μg ml^{-1} purified h-MAdCAM-1/Fc in coating buffer (PBS, 10 mM $NaHCO_3$, pH 9.0) for 1 h at 37 °C, followed by 2% (w/v) human serum albumin in coating buffer for 1 h at 37 °C to block nonspecific binding sites[18]. The dish was assembled as the lower wall of a parallel plate flow chamber and mounted on the stage of an inverted phase-contrast microscope[35].

Cells were washed twice with Ca^{2+}- and Mg^{2+}-free HBSS, 10 mM HEPES, pH 7.4, 5 mM EDTA, 0.5% (w/v) BSA and resuspended at 5×10^6 ml^{-1} in buffer A (Ca^{2+}- and Mg^{2+}-free HBSS, 10 mM HEPES, 0.5% (w/v) BSA) and kept at room temperature. Cells were diluted (293T transfectant, 1×10^6 ml^{-1}; K562 stable transfectants, 5×10^5 ml^{-1}) in buffer A containing different divalent cations immediately before infusion in the flow chamber using a syringe pump. Microscope images were recorded for later analysis.

Cells were allowed to accumulate for 30 s at 0.3 dyn cm^{-2}. Then, shear stress was increased every 10 s from 1 dyn cm^{-2} up to 32 dyn cm^{-2}, in two-fold increments. The number of cells remaining bound at the end of each 10-s interval was determined. Rolling velocity at each shear stress was calculated from the average distance traveled by rolling cells in 3 s. To avoid confusing rolling with small amounts of movement due to tether stretching or measurement error, a velocity of 2 μm s^{-1}, which corresponds to a movement of 1/2 cell diameter during the 3 s measurement interval, was the minimum velocity required to define a cell as rolling instead of firmly adherent[23].

ACKNOWLEDGMENTS

We thank D.J. Erle and M.J. Briskin for providing wild-type human integrin β_7 cDNA and $\alpha_4\beta_7$ K562 stable transfectant and human MAdCAM-1/Fc, respectively. This work was supported by a grant from the US National Institutes of Health.

COMPETING INTERESTS STATEMENT

The authors declare that they have no competing financial interests.

Received 6 June; accepted 15 September 2003
Published online at http://www.nature.com/naturestructuralbiology/

1. Shimaoka, M., Takagi, J. & Springer, T.A. Conformational regulation of integrin structure and function. *Annu. Rev. Biophys. Biomol. Struct.* **31**, 485–516 (2002).
2. Emsley, J., Knight, C.G., Farndale, R.W., Barnes, M.J. & Liddington, R.C. Structural basis of collagen recognition by integrin α2β1. *Cell* **101**, 47–56 (2000).
3. Beglova, N., Blacklow, S.C., Takagi, J. & Springer, T.A. Cysteine-rich module structure reveals a fulcrum for integrin rearrangement upon activation. *Nat. Struct. Biol.* **9**, 282–287 (2002).
4. Shimaoka, M. *et al.* Structures of the αL I domain and its complex with ICAM-1 reveal a shape-shifting pathway for integrin regulation. *Cell* **112**, 99–111 (2003).
5. Takagi, J., Petre, B.M., Walz, T. & Springer, T.A. Global conformational rearrangements in integrin extracellular domains in outside-in and inside-out signaling. *Cell* **110**, 599–611 (2002).
6. Takagi, J., Strokovich, K., Springer, T.A. & Walz, T. Structure of integrin α5β1 in complex with fibronectin. *EMBO J.* **22**, 4607–4615 (2003).
7. Xiong, J.-P. *et al.* Crystal structure of the extracellular segment of integrin αVβ3. *Science* **294**, 339–345 (2001).
8. Xiong, J.P. *et al.* Crystal structure of the extracellular segment of integrin αVβ3 in complex with an Arg-Gly-Asp ligand. *Science* **296**, 151–155 (2002).
9. Marlin, S.D. & Springer, T.A. Purified intercellular adhesion molecule-1 (ICAM-1) is a ligand for lymphocyte function-associated antigen 1 (LFA-1). *Cell* **51**, 813–819 (1987).
10. Gailit, J. & Ruoslahti, E. Regulation of the fibronectin receptor affinity by divalent cations. *J. Biol. Chem.* **263**, 12927–12932 (1988).
11. Dransfield, I., Cabañas, C., Craig, A. & Hogg, N. Divalent cation regulation of the

function of the leukocyte integrin LFA-1. *J. Cell Biol.* **116**, 219–226 (1992).
12. Staatz, W.D., Rajpara, S.M., Wayner, E.A., Carter, W.G. & Santoro, S.A. The membrane glycoprotein Ia-IIa (VLA-2) complex mediates the Mg^{++}-dependent adhesion of platelets to collagen. *J. Cell Biol.* **108**, 1917–1924 (1989).
13. Mould, A.P., Akiyama, S.K. & Humphries, M.J. Regulation of integrin α5β1-fibronectin interactions by divalent cations. *J. Biol. Chem.* **270**, 26270–26277 (1995).
14. Hu, D.D., Hoyer, J.R. & Smith, J.W. Ca^{2+} suppresses cell adhesion to osteopontin by attenuating binding affinity for integrin αvβ3. *J. Biol. Chem.* **270**, 9917–9925 (1995).
15. Leitinger, B., McDowall, A., Stanley, P. & Hogg, N. The regulation of integrin function by Ca^{2+}. *Biochim. Biophys. Acta* **1498**, 91–98 (2000).
16. Berlin, C. *et al.* α4 integrins mediate lymphocyte attachment and rolling under physiologic flow. *Cell* **80**, 413–422 (1995).
17. Alon, R. *et al.* The integrin VLA-4 supports tethering and rolling in flow on VCAM-1. *J. Cell Biol.* **128**, 1243–1253 (1995).
18. de Chateau, M., Chen, S., Salas, A. & Springer, T.A. Kinetic and mechanical basis of rolling through an integrin and novel Ca^{2+}-dependent rolling and Mg^{2+}-dependent firm adhesion modalities for the α4β7–MAdCAM-1 interaction. *Biochemistry* **40**, 13972–13979 (2001).
19. Springer, T.A. Predicted and experimental structures of integrins and β-propellers. *Curr. Opin. Struct. Biol.* **12**, 802–813 (2002).
20. Pujades, C. *et al.* Defining extracellular integrin α chain sites that affect cell adhesion and adhesion strengthening without altering soluble ligand binding. *Mol. Biol. Cell* **8**, 2647–2657 (1997).
21. Knorr, R. & Dustin, M.L. The lymphocyte function-associated antigen 1 I domain is a transient binding module for intercellular adhesion molecule (ICAM)-1 and ICAM-1 in hydrodynamic flow. *J. Exp. Med.* **186**, 719–730 (1997).
22. Lu, C., Shimaoka, M., Zang, Q., Takagi, J. & Springer, T.A. Locking in alternate conformations of the integrin αLβ2 I domain with disulfide bonds reveals functional relationships among integrin domains. *Proc. Natl. Acad. Sci. USA* **98**, 2393–2398 (2001).
23. Salas, A., Shimaoka, M., Chen, S., Carman, C.V. & Springer, T.A. Transition from rolling to firm adhesion is regulated by the conformation of the I domain of the integrin LFA-1. *J. Biol. Chem.* **277**, 50255–50262 (2002).
24. Berlin, C. *et al.* α4β7 integrin mediates lymphocyte binding to the mucosal vascular addressin MAdCAM-1. *Cell* **74**, 185–195 (1993).
25. Bargatze, R.F., Jutila, M.A. & Butcher, E.C. Distinct roles of L-selectin and integrins α4β7 and LFA-1 in lymphocyte homing to Peyer's patch-HEV *in situ*: the multistep model confirmed and refined. *Immunity* **3**, 99–108 (1995).
26. Briskin, M.J., McEvoy, L.M. & Butcher, E.C. MAdCAM-1 has homology to immunoglobulin and mucin-like adhesion receptors and to IgA1. *Nature* **363**, 461–464 (1993).
27. Chang, K.-C., Tees, D.F. & Hammer, D.A. The state diagram for cell adhesion under flow: leukocyte rolling and firm adhesion. *Proc. Natl. Acad. Sci. USA* **97**, 11262–11267 (2000).
28. Harding, M.M. Geometry of metal-ligand interactions in proteins. *Acta Crystallogr. D* **57**, 401–411 (2001).
29. Tidswell, M. *et al.* Structure-function analysis of the integrin β_7 subunit: Identification of domains involved in adhesion to MAdCAM-1. *J. Immunol.* **159**, 1497–1505 (1997).
30. Lu, C. & Springer, T.A. The α subunit cytoplasmic domain regulates the assembly and adhesiveness of integrin lymphocyte function-associated antigen-1 (LFA-1). *J. Immunol.* **159**, 268–278 (1997).
31. Lu, C., Oxvig, C. & Springer, T.A. The structure of the β-propeller domain and C-terminal region of the integrin αM subunit. *J. Biol. Chem.* **273**, 15138–15147 (1998).
32. Kassner, P.D. & Hemler, M.E. Interchangeable α chain cytoplasmic domains play a positive role in control of cell adhesion mediated by VLA-4, a β_1 integrin. *J. Exp. Med.* **178**, 649–660 (1993).
33. Lazarovits, A.I. *et al.* Lymphocyte activation antigens: I. A monoclonal antibody, anti-act I, defines a new late lymphocyte activation antigen. *J. Immunol.* **133**, 1857–1862 (1984).
34. Schweighoffer, T. *et al.* Selective expression of integrin α4β7 on a subset of human $CD4^+$ memory T cells with hallmarks of gut-trophism. *J. Immunol.* **151**, 717–729 (1993).
35. Lawrence, M.B. & Springer, T.A. Leukocytes roll on a selectin at physiologic flow rates: distinction from and prerequisite for adhesion through integrins. *Cell* **65**, 859–873 (1991).